9-12-2007

Oxygen Measurement via Phosphorescence: Reaction of Sodium Dithionite with Dissolved Oxygen

Zhimin Tao
State University of New York

Jerry Goodisman
Syracuse University

Abdul-Kader Souid
State University of New York

Oxygen Measurement via Phosphorescence: Reaction of Sodium Dithionite with Dissolved Oxygen

Zhimin Tao,[†] Jerry Goodisman,*[,‡] and Abdul-Kader Souid*[,†]

Department of Pediatrics, State University of New York, Upstate Medical University, 750 East Adams Street, Syracuse, New York 13210 and Department of Chemistry, Syracuse University, CST, 1-014, Syracuse, New York 13244

Received: September 12, 2007

A homemade instrument for the measurement of oxygen concentration in aqueous solutions measures the decay rate of the phosphorescence of a Pd-porphyrin complex (phosphor) dissolved in the solution, which is flashed every 0.1 s with 630 nm light. The concentration of O_2 is a linear function of the decay rate. The instrument is used to study the reaction of dithionite ($S_2O_4^{2-}$) with O_2 at 25 °C and 37 °C. It is found that the ratio of dithionite to oxygen consumed in the reaction is 1.2 ± 0.2 at 25 °C and 1.7 ± 0.1 at 37 °C, suggesting a temperature-dependent stoichiometry. At both temperatures, the initial rate of O_2 consumption, $-d[O_2]/dt$, is found to be 1/2 order in $S_2O_4^{2-}$ and first order in O_2. This finding is consistent with a previously proposed mechanism: $S_2O_4^{2-} \leftrightarrow 2SO_2^-$ comes to a rapid equilibrium, and SO_2^- reacts with O_2 in the rate-determining step.

1. Introduction

Measurement of O_2 concentration based on the quenching of the phosphorescence of Pd (II)-meso-tetra-(4-sulfonatophenyl)-tetrabenzoporphyrin (Pd phosphor) was introduced by Wilson and his co-workers.[1−4] This method allows accurate and sensitive determination of $[O_2]$ in biological systems.[1] Using a homemade instrument, we recently used this method to monitor cellular respiration (mitochondrial O_2 consumption) under various conditions.[5−7] The instrument records and analyzes the phosphorescence profile (emitted light intensity vs time) of the Pd phosphor, which is excited with a flash of 630 nm light.[1−4] Since O_2 quenches the phosphorescence of this probe, the decay constant of emitted light depends linearly on $[O_2]$.[5,6]

The stoichiometry and kinetics of the reaction of dithionite with dissolved oxygen is studied here using this instrument, which we briefly describe below, as well as the analysis of experimental results. We then report our measurements of stoichiometry and rate constants for the reaction of sodium dithionite ($Na_2S_2O_4$) with dissolved O_2.

Sodium dithionite ($Na_2S_2O_4$), also known as sodium hydrosulfite or hyposulfite, has been reported to decompose in aqueous solutions. Under aerobic conditions, dithionite ion $S_2O_4^{2-}$ reduces O_2 to the −2 oxidation state rapidly,[8] producing bisulfate and/or bisulfite. The overall reaction is written as:

$$S_2O_4^{2-} + O_2 + H_2O \rightarrow HSO_3^- + HSO_4^- \qquad (1)$$

(implying equal amounts of bisulfite and bisulfate are produced, as first reported).[9,10] Two reactions are actually possible:

$$S_2O_4^{2-} + \frac{1}{2}O_2 + H_2O \rightarrow 2HSO_3^- \qquad (2)$$

$$S_2O_4^{2-} + \frac{3}{2}O_2 + H_2O \rightarrow 2HSO_4^- \qquad (3)$$

The ratio between bisulfite and bisulfate depends on the relative contributions of reactions 2 and 3. The initial steps of the reaction may involve eqs 4 and 5:

$$S_2O_4^{2-} \leftrightarrow 2SO_2^- \qquad (4)$$

$$SO_2^- + O_2 \rightarrow \text{products} \qquad (5)$$

with eq 5 being followed by a series of further reactions.[9]

Raman spectroscopy[11] and X-ray[12] studies on $S_2O_4^{2-}$ suggested a planar D_{2h} structure, which has one S−S bond in the center and two S−O bonds with different lengths in each half-anion. This is consistent with eq 4, which shows dissociation of $S_2O_4^{2-}$ into two units of SO_2^-. In addition, a mechanism for eq 5, which explained the equal amounts of bisulfate and bisulfate, was proposed by Rinker et al. The first step in eq 5 was

$$\bullet SO_2^- + O_2 \rightarrow SO_2 + \bullet O_2^- \qquad (6)$$

with several other radicals involved in subsequent steps.[9] Nonetheless, there is no evidence for or against this mechanism.

Depending on which step is rate-determining in eqs 4 and 5, different kinetic schemes result. Some authors[10] reported zero-order with O_2, implying the forward reaction in eq 4 is rate-determining; this also predicts the reaction to be first-order with respect to $S_2O_4^{2-}$. Other researchers[9] claimed that the equilibrium in eq 4 is very rapid, and thus, eq 5 is the rate-controlling step; this predicts first-order kinetics with respect to O_2 and 1/2-order with respect to $S_2O_4^{2-}$. However, the rate-controlling

* Corresponding authors. Phone: 315-443-3035. Fax: 315-443-4070. E-mail: goodisma@syr.edu (J.G.) and Phone: 315-464-5294. Fax: 315-464-7238. E-mail: souida@upstate.edu (A.-K.S.).
[†] State University of New York.
[‡] Syracuse University.

10.1021/jp710176z CCC: $40.75
Published on Web 01/30/2008

step, like the ratio of bisulfate and bisulfite in the final products, may depend on temperature and relative amounts of $S_2O_4^{2-}$ and O_2.

Only a few studies[13] of the reaction of $S_2O_4^{2-}$ with O_2 in solutions have been reported lately, and they do not address the mechanism. Most investigations monitored changes in the spectroscopic absorbance of $S_2O_4^{2-}$ ($\lambda_{max} = 315$ nm). Here, we investigate the stoichiometry and kinetics of this reaction by tracking O_2 consumption using our O_2 analyzer. The results suggest the stoichiometry for the overall reaction is temperature-sensitive. The kinetics is shown to be 1/2-order with respect to $S_2O_4^{2-}$ and first-order with respect to O_2, showing that eq 5 is the rate-limiting step.

2. Experimental Section

2.1. Materials. Pd (II) complex of meso-tetra-(4-sulfonatophenyl)-tetrabenzoporphyrin (Pd phosphor, sodium salt) was obtained from Porphyrin Products (Logan, UT). Pd phosphor solution (2.5 mg/mL = 2 mM) was prepared in dH_2O and stored at −20 °C in small aliquots. D(+)glucose anhydrous (Cat # 346351, lot #D00003205) was purchased from Calbiochem (La Jolla, CA). Glucose oxidase (from *Aspergillus niger*; 1400 units/mL in 100 mM sodium acetate, pH ~ 4.0) was purchased from Sigma-Aldrich (St. Louis, MO). Sodium dithionite (MW 174.11) was purchased from Fluka, U.K. Working solutions (0.5−1.0 M) were freshly made in dH_2O under argon shield. Bovine serum albumin (BSA) was purchased from Sigma-Aldrich.

2.2. Instrument. An optical instrument was built to measure the phosphorescence of Pd phosphor.[1−4] The probe was excited by light pulses (10 per s) that peaked at 625 nm (OTL630A-5−10-66-E, Opto Technology, Inc., Wheeling, IL). Duration of a pulse was 50−100 μs. Emitted phosphorescence was isolated by a filter centered at 800 nm and passed through a Hamamatsu photomultiplier tube (# 928). Five microseconds after each flash, the resulting phosphorescence was digitized at 1 MHz by the ultrahigh-speed PCI-DAS4020/12 analog input board (Measurement Computing Corporation, Norton, MA). DASYlab (Measurement Computing Corporation, Norton, MA) was used for data acquisition.

Samples (final volume, 1.0 mL with dH_2O) containing 2 μM Pd-phosphor and 0.5% bovine fat-free albumin were placed in 1 mL glass vials. Serum albumin binds the Pd-phosphor molecules and protects them from external chemical disturbance, such as changes in pH. The vials were sealed and placed in the instrument for O_2 measurement. Mixing was accomplished with the aid of parylene-coated stirring bars.

2.3. Data Analysis. A typical phosphorescence intensity profile, for air-saturated dH_2O to which 200 μM $S_2O_4^{2-}$ has been added, is shown in Figure 1. Dithionite reacts rapidly with dissolved O_2 and, as shown below, 200 μM $S_2O_4^{2-}$ removes more than half of the O_2 in air-saturated water. The data were analyzed by a computing program (C^{++} language, Table 1) that calculated the phosphorescence lifetime (τ) and decay constant ($1/\tau$), from which $[O_2]$ can be determined using eq 7

$$\frac{1}{\tau} = \frac{1}{\tau_0} + k_q[O_2] \tag{7}$$

where the values of $1/\tau_0$ (10087 ± 156 s^{-1}) and k_q (96.1 ± 1.2 μM^{-1} s^{-1}) were established by calibration.[5]

In the phosphorescence profile shown in Figure 1, the flash goes on at $t = t_0 \sim 0.078548$ s, stays on with a constant intensity until $t = t_1 \sim 0.078626$ s, and then goes off, so that the flash duration is ~78 μs. Since phosphorescence is a first-order

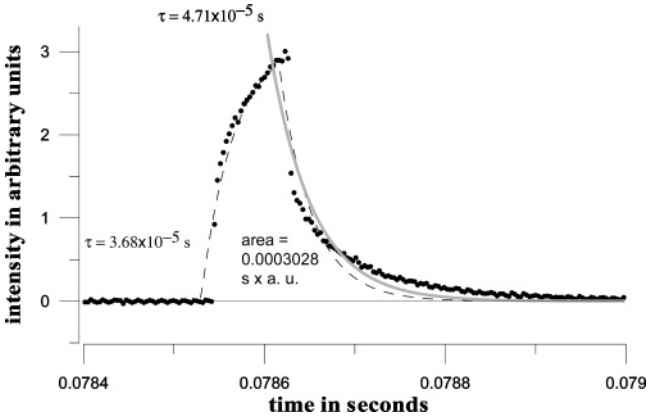

Figure 1. Phosphorescence profile of dH_2O containing 2.0 μM Pd phosphor, 0.5% albumin, and 200 μM $S_2O_4^{2-}$. One can measure the lifetime τ from the area and peak height of the profile, by fitting the profile to the theoretical form (dashed line), or by fitting the decreasing part to an exponential (solid gray line).

process, the phosphorescence intensity (I) is proportional to the number of phosphor molecules in the excited state. This population decays with time and is pumped by the flash at a constant rate k'. Thus, $I = 0$ for $t < t_0$, and

$$\frac{dI}{dt} = k' - \frac{I}{\tau} \qquad t_0 < t < t_1$$

which integrates to

$$I = k'\tau[1 - e^{-(t-t_0)/\tau}] \tag{8}$$

For $t > t_1$ (lamp off),

$$I = c\, e^{-(t-t_1)/\tau} \tag{9}$$

where c is the maximum intensity (at t_1); that is,

$$c = k'\tau[1 - e^{-(t_1 - t_0)/\tau}]$$

The value of c is proportional to τ only if $t_1 - t_0 \gg \tau$. There are several ways of obtaining τ from an intensity profile like the one in Figure 2, and we compare them here.

From direct reading of the experimental intensities (solid dots), one finds $t_0 = 0.0785482$ s, $t_1 = 0.0786263$ s, maximum intensity $c = 3.00293$ arbitrary units, and total area under the curve,

$$A = \int_{t_0}^{\infty} I\, dt = k'\tau(t_1 - t_0)$$

= 0.0003028 arbitrary units × s (by numerical integration). If these data followed the theoretical equation exactly, the ratio of the area to the height c would be

$$\frac{A}{c} = \frac{k'\tau(t_1 - t_0)}{k'\tau\{1 - \exp[(t_0 - t_1)/\tau]\}} = 1.0083 \times 10^{-4}\ \text{s}$$

so that $\exp[(t_0 - t_1)/\tau] = 1 - 0.77457$ and $\tau = 5.24 \times 10^{-5}$ s. This method for extracting τ has the advantage of using all of the experimental data and does not necessitate determining k' separately. The disadvantages include involving calculations in which accuracy is lost because $(c/A)(t_1 - t_0)$ is often close to 1 and requiring an arbitrary choice of where to truncate the area integration. An alternative is to fit the experimental data to the theoretical form using nonlinear least-squares. The best fit (dashed curve in Figure 2) corresponds to $t_0 = 0.0785337$ s, t_1

TABLE 1: C^{++} Language Program for Computing $1/\tau$

```
#include <stdio.h>
#include <stdlib.h>
#include <math.h>
#include <time.h>
#include <malloc.h>

typedef struct DATUM
{
        struct DATUM *prior;
        double time;
        float intensity;
        double lny;
        struct DATUM *next;
}DATUM;

#define FILENAME "experimental data.ASC" //data file name
#define THRESHOLD 0.05 //data dropping threshold
#define STEPLENGTH 0.00001 //time interval
#define NOISEAVER 10 //average in every second

#define MAXIAVER 3 //use average of last # as maximum
#define MAXIMATIME 0.00005
#define MAXIMAINT 1.2
/* maximal point: (p->next->time)-(p->time)<MAXIMATIME
& (p->intensity)-(p-)next->intensity)>MAXIMAINT */

#define PERIODTIME 0.001
#define PERIODINT 0.1
/* period point: (p->next->time)-(p->time)>PERIODTIME
& abs((p->next->intensity)-(p->intensity))<PERIODINT */
#define MAXPERIOD 0.0001

FILE *fp;

void main()
{
        float y=0;
        double
t=0,mx=0,my=0,mxy=0,mxx=0,k=0,ka=0,ta=0,ym=0,yma=0;
        int count=0; //period counter
        int n=0; //average counter
        DATUM *p,*p1,*p2,*head;

        srand((unsigned)time(NULL));

//read data & selection start

        fp=fopen(FILENAME,"r");

        head=(DATUM *)malloc(sizeof(DATUM));
        p1=head;
        p=p1;

        while(fscanf(fp,"%f",&y)==1)
        {
                if(y>THRESHOLD)
                {
                        p1=p;
                        p->time=t;
                        p->intensity=y;
                        p->lny=log(y);
                        p->next=(DATUM
*)malloc(sizeof(DATUM));
                        p=p->next;
                        p->prior=p1;
//                      printf("%f\n",t);
//                      getchar();
                }
                t=t+STEPLENGTH;
        }
        p1->next=head;
        head->prior=p1;
        free(p);

        fclose(fp);

        printf("finish selection!\n");
///*
        fp=fopen("selected.dat","w");
        p=head;
        while(p->next!=head)
        {
                fprintf(fp,"%f          %f\n",p->time,p->intensity);
                p=p->next;
        }
        fclose(fp);
//*/
//selection finish

//grouping & fit start
///*
        printf("start fitting!\n");

        fp=fopen("result.dat","w");

        p=head;

        n=0;
                yma=0;
                ka=0;
                ta=0;
                ym=0;

        while(p->next!=head)
        {
                count=0;
                mx=0;
                my=0;
                mxy=0;
                mxx=0;
                while((((p->intensity)-(p->next-
>intensity))<MAXIMAINT)||(((p->next->time)-(p-
>time))>MAXIMATIME))
                {
                        p=p->next;
                        if(p->next==head)
                                goto
finish;
                }
                p1=p->next;//p1 is start of a
period
                p2=p;
                while(count<MAXIAVER)
                {
                        ym+=p2->intensity;
                        p2=p2->prior;
                        count++;
                }
                ym=ym/MAXIAVER;
                p2=p1;
                count=0;
                while(((p2->next->time)-(p2-
>time))<PERIODTIME)
                {
                        count++;
                        mx+=(p2->time);
                        my+=(p2->lny);
                        mxx+=((p2-
>time)*(p2->time));
                        mxy+=((p2-
>time)*(p2->lny));
                        p2=p2->next;
                        if(((p2->time)-(p1-
>time)>MAXPERIOD))
                                break;
                        if(p2->next==head)
                                goto
finish;
                }
                k=(count*mxy-
mx*my)/(count*mxx-mx*mx);
                if(k<0)
                        k=0-k;
                n++;
                ka+=k;
                yma+=ym;
                ta+=p1->time;
                if(n==NOISEAVER)
                {
                        ka=ka/NOISEAVER;

        yma=yma/NOISEAVER;
                        ta=ta/NOISEAVER;
                        fprintf(fp,"%f
        %f      %f      %f
                        %f      %f      %f\n",p1-
>time,p2->time,k,ym,ta,ka,yma);
                        n=0;
                        ka=0;
                        ta=0;
                        yma=0;
                }
                else
                        fprintf(fp,"%f
        %f      %f      %f\n",p1->time,p2-
>time,k,ym);
                if(p2->next==head)
                        goto finish;
                p=p2;
                printf("1 period!\n");
        }

finish:  fclose(fp);
//*/

//grouping & fit finish

}
```

$= 0.0786150$ s, maximum height $c = 2.84994$ arbitrary units, and peak area $= 0.0002714$ arbitrary units $\times$ s (from integration of eqs 8 and 9 to $t \rightarrow \infty$). Then $A/c = 9.523 \times 10^{-5}$ s, so that $\exp[(t_0 - t_1)/\tau] = 1 - 0.90309$ and $\tau = 3.68 \times 10^{-5}$ s. The fitting process is much more tedious than direct measurement, and the quality of the fit (see Figure 2) is only fair, so that the value of τ is inaccurate.

Fortunately, a simpler and more accurate method is available: after locating the position of the maximum, one fits the decreasing part of the profile to an exponential function. The fit, shown as a solid gray line in Figure 1, gives $\tau = 4.71 \times 10^{-5}$ s, reasonably close to what is obtained by direct analysis of all the data. The exponential fit is more reliable; although it uses less of the data, it requires determination of only one parameter, the decay rate ($1/\tau$). This method is easily implemented in the computer program, and we therefore use the exponential fit to determine the value of τ.

Furthermore, we will always be comparing τ values after calibration. The sampling was done at 307 200 Hz. Since the lamp flashes every 0.1 s, the duration of the flash is 78 μs, and

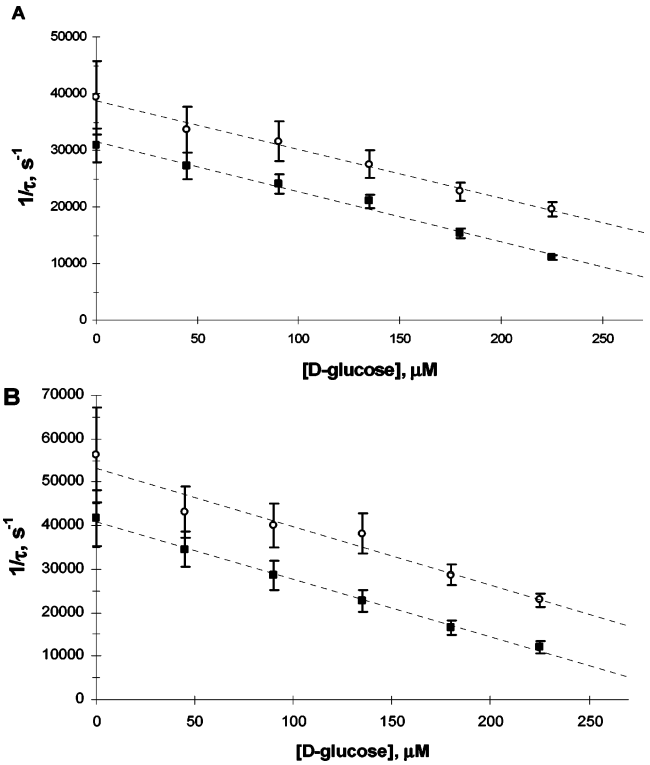

Figure 2. Measured values of $1/\tau$ for solutions containing glucose oxidase, with (squares) or without (open circles) dithionite, after addition of D-glucose. Panel A, 25 °C; panel B, 37 °C. The slopes of the best-fit lines (dotted) are identical with and without dithionite, showing that the measurement of $[O_2]$ by phosphorescence decay is not affected by dithionite.

the decay time τ is about 40 μs; the useful data from each flash involves fewer than 100 points, and >99.8% of the readings are zero and of no interest. The analysis program removes all zero or zero-like readings by setting a data-dropping threshold (e.g., 0.05), producing a sawtooth intensity-versus-time plot, composed of a number of profiles like that of Figure 1. It is necessary to find the maximum in each profile and fit the points after the maximum to an exponential. The Microsoft Visual C^{++} program (Table 1) combines these tasks by screening the data stream for maxima with intensities greater than 0.05, noting the time of each maximum (t_1) and keeping only data declining from the peak but above the data-dropping threshold within 0.1 s. This produces 10 decay curves per second, each of which is fit to an exponential function.

The possibility that the phosphor is affected by the dithionite or its oxidation products[14] was also investigated, by measuring the glucose oxidase-catalyzed oxidation of glucose at 25 °C and 37 °C (Figure 2). The overall reaction of glucose ($C_6H_{12}O_6$) with O_2 produces gluconic acid ($C_6H_{12}O_7$) and H_2O_2,

$$\text{glucose} + O_2 + H_2O \rightarrow \text{gluconic acid} + H_2O_2$$

The reaction mixtures (in dH_2O) contained 2 μM Pd phosphor, 0.5% albumin, and glucose oxidase (7.0 units/mL) with or without 1.0 mM dithionite. The solutions were stirred and equilibrated with air for 30 min. One milliliter of each solution was then placed in a sealed vial for $[O_2]$ measurement at 25 °C (panel A) and 37 °C (panel B). O_2 was consumed rapidly on injection of 45, 90, 135, 180, and 225 μM (final concentrations) D-glucose. Measured $1/\tau$ (in s^{-1}) decreased as [D-glucose] increased; the best linear fits are shown.

At 25 °C (Figure 2A), the slope without dithionite (circles) was -86.065 ± 4.479 ($r^2 > 0.99$) and with dithionite (squares) -87.581 ± 4.778 ($r^2 > 0.99$). At 37 °C (Figure 2B), the slope without dithionite (circles) was -134.72 ± 16.19 ($r^2 > 0.95$) and with dithionite (squares) -132.13 ± 3.99 ($r^2 > 0.99$). Thus, the effect of dithionite and its oxidation products on the Pd-phosphor at 25 °C and 37 °C was negligible. The curves in the presence of dithionite were lower because of less dissolved O_2 in these solutions.

3. Results and Discussion

3.1. Experimental Results. Figures 3 and 4 show representative plots of the reciprocal of the measured decay constant τ (+ signs) obtained in successive measurements at 25 °C (Figure 3) and 37 °C (Figure 4). Each plot corresponds to an experiment in which dithionite was added to air-saturated water at the concentration shown in the plot label. Here, $1/\tau$ is plotted versus elapsed time. Since, according to eq 7, $1/\tau$ is a linear function of $[O_2]$, these are essentially plots of $[O_2]$ versus time. The rapid decline in $[O_2]$ when $S_2O_4^{2-}$ is injected is evident.

For each plot, the values of $1/\tau$ before and after the drop in $[O_2]$, $1/\tau_b$ and $1/\tau_a$, were obtained by averaging 100−200 measurements. The value of $1/\tau_b$ should correspond to the oxygen concentration in air-saturated dH_2O, which is 267 μM at 25 °C and 225 μM at 37 °C.[14] When $[S_2O_4^{2-}] > 500$ μM, the value of $1/\tau_a$ corresponds to total depletion of O_2; that is $1/\tau_a = 1/\tau_0$. From the values of $1/\tau_b$ and $1/\tau_a$, we obtain information about the stoichiometry of the overall reaction (see below). From the shape of the experimental curve, we obtain information about the kinetics and rate constant of the reaction. It can be seen, for instance, that the drop in $1/\tau$ is rapid and mostly linear, suggesting a reaction which is zero-order in O_2. However, in many plots, one can also note a tail or rounding-off in the experimental data as $1/\tau$ approaches $1/\tau_0$, suggesting either that the plots are actually curved or that the rate-determining step is no longer zero-order when $[O_2]$ drops below a certain level.

The solid lines in Figures 3 and 4 are fits of the experimental data to the four-parameter function

$$\begin{aligned} \frac{1}{\tau} &= \frac{1}{\tau_b} \qquad t < t_b \\ &= \frac{1}{\tau_a} + \left(\frac{1}{\tau_b} - \frac{1}{\tau_a}\right) \exp[-C(t - t_b)] \qquad t \geq t_b \end{aligned} \tag{10}$$

with the values of the parameters C and t_b found by minimizing the sum of the square deviations of eq 10 from experimentally measured $1/\tau$, $1/\tau_b$ and $1/\tau_a$ having been previously determined. One obtains a first-order rate constant for oxygen depletion by multiplying $-d(1/\tau)/dt$ by τ/k_q, where $k_q = 96.1$ μM^{-1} s^{-1}. Further, one obtains the initial rate (or zero-order rate constant) from the value of $-d(1/\tau)/dt$ at $t = t_b$:

$$r = \left(\frac{1}{\tau_b} - \frac{1}{\tau_a}\right)\frac{C}{k_q} \tag{11}$$

We have also fitted (not shown) the experimental data to the four-parameter function,

$$\begin{aligned} 1/\tau &= 1/\tau_b \qquad t < t_b \\ &= 1/\tau_b + (t - t_b)(1/\tau_a - 1/\tau_b)/(t_a - t_b) \qquad t_b \leq t \leq t_a \\ &= 1/\tau_a \qquad t > t_a \end{aligned} \tag{12}$$

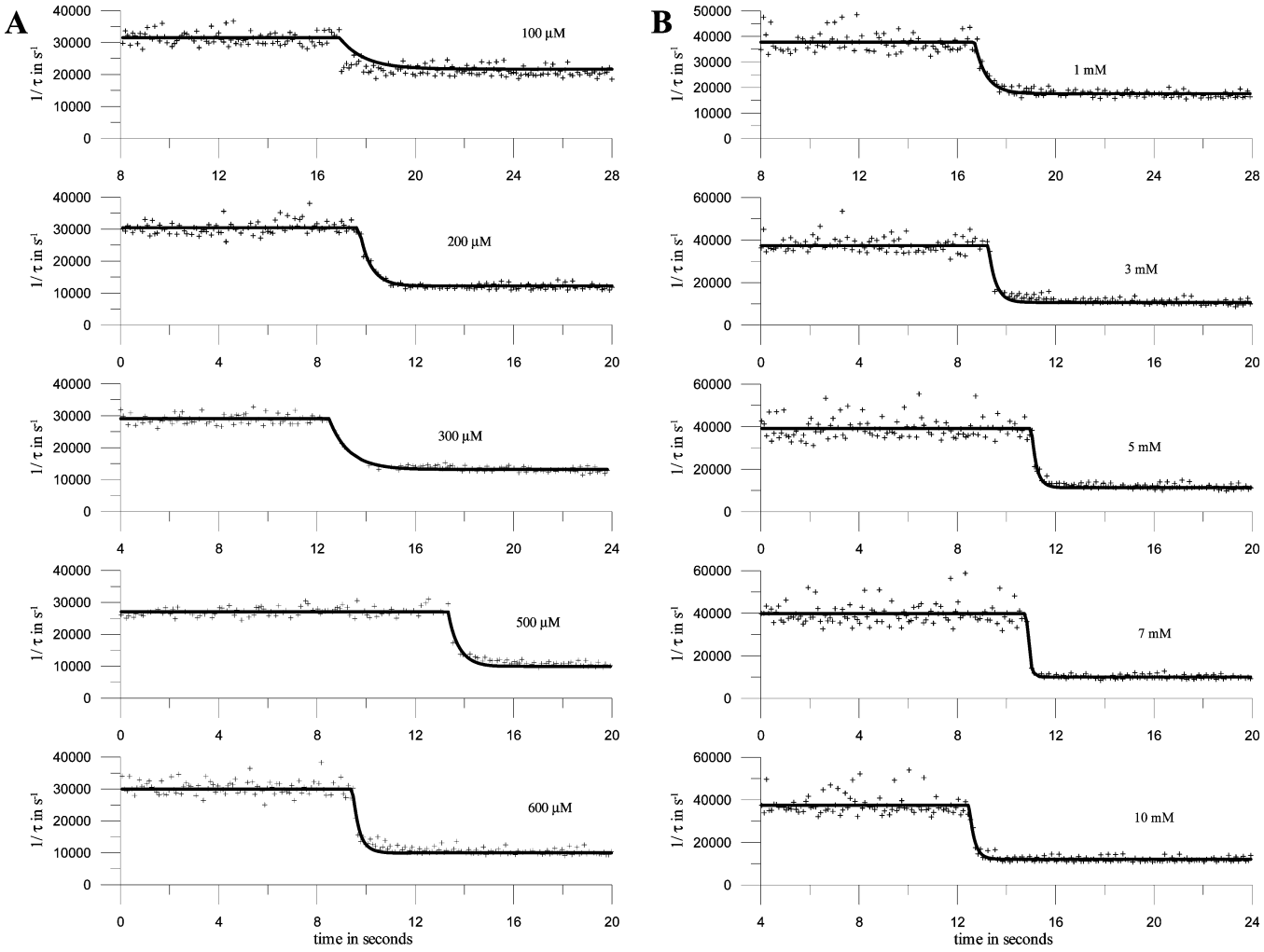

Figure 3. Representative plots (+ signs) of $1/\tau$ vs time obtained by reaction of $S_2O_4^{2-}$ with dissolved O_2 at 25 °C. The reaction (in dH_2O) contained 2.0 μM Pd phosphor, 0.5% albumin, and 50 to 600 μM (A) or 1−10 mM $S_2O_4^{2-}$ (B). The rapid decrease in $1/\tau$ when $S_2O_4^{2-}$ is added corresponds to its reaction with O_2. The solid lines are best fits to a horizontal line followed by a decreasing exponential.

From eq 12, the zero-order rate constant or reaction rate is

$$r = k_0 = \frac{1}{k_q}\left(\frac{1}{\tau_b} - \frac{1}{\tau_a}\right)\frac{1}{(t_a - t_b)} \qquad (13)$$

The fit to eq 10 is somewhat better than the fit to eq 12 because eq 10 takes into account the curvature in the plots as $1/\tau$ approaches $1/\tau_a$.

3.2. Stoichiometry of the Reaction of $S_2O_4^{2-}$ with O_2. At 25 °C, 22 data sets with various concentrations of $S_2O_4^{2-}$ below 1.0 mM were obtained. For some of them, the values of $1/\tau_a$ are plotted versus $[S_2O_4^{2-}]$ in Figure 5A, where each error bar is the standard deviation for one determination of $1/\tau_a$. Figure 5B, similarly, shows the results of some of the measurements at 37 °C.

It is expected that $[O_2]$ after $S_2O_4^{2-}$ addition (obtained from τ_a) will decrease linearly with $d = [S_2O_4^{2-}]$ for $d < s[O_2]_0$, where s is the ratio of $S_2O_4^{2-}$ consumed to $[O_2]$ consumed, until $d = s[O_2]_0$, $[O_2]_0$ being the original $[O_2]$. For $[S_2O_4^{2-}] > s[O_2]$, $1/\tau_a$ should equal $1/\tau_0$, since all of the oxygen has been reduced. The broken line in Figure 5A is the best fit of all 22 data points to the 3-parameter function

$$1/\tau = \alpha + \beta d, \quad d < \delta; \qquad 1/\tau = \gamma, \quad d > \delta \qquad (14)$$

where $\alpha + \beta\delta = \gamma$. This best fit has $\alpha = 28\,844$ s^{-1}, $\beta = -54.0$ s^{-1} μM^{-1}, $\delta = 312.3$ μM, and $\gamma = 11971$ s^{-1}. Since $[O_2]_0 = 267.2$ μM, $s = 1.167 \pm 0.201$ (error from linear fit). This result is consistent with eq 1 but suggests that s may be slightly greater than 1.

A similar analysis was made of the 28 data sets from measurements at 37 °C with dithionite concentrations below 1.0 mM. The values of $1/\tau_a$ are plotted versus $[S_2O_4^{2-}]$ in Figure 5B, where each error bar is the standard deviation for one determination of $1/\tau_a$. The dashed line in Figure 5B is the best fit to eq 14, using all 28 values of $1/\tau_a$. In this case, $\alpha = 41745$ s^{-1}, $\beta = -80.4$ s^{-1} μM^{-1}, $\delta = 384.2$ μM, and $\gamma = 10823$ s^{-1}. Since $[O_2]_0 = 225.4$ μM, $s = 1.705 \pm 0.134$ (error from linear fit). This result is significantly different from what is implied by eq 1 and shows that eq 2 occurs more often than eq 3 at the higher temperature.

3.3. Kinetics of the Reaction of $S_2O_4^{2-}$ with O_2. In these experiments, $S_2O_4^{2-}$ was added to a sample of air-saturated dH_2O containing Pd phosphor without interrupting the measurement of τ, and the measured values of $1/\tau$, which depends linearly on $[O_2]$, were plotted versus t. The data sets studied resemble those in Figures 3 and 4. The plots for 25 °C (Figure 3A,B) show a mostly linear decrease in $1/\tau$ from $t = t_b$ to $t = t_a$; that is, the decrease is initially linear and deviates from linearity for $1/\tau$ below about 15 000 s^{-1}; according to eq 7, this corresponds to $[O_2] < 40$ μM. In the plots for 37 °C (Figure 4A,B), the decrease is much faster, corresponding to faster rates at the higher temperature. Where $d[O_2]/dt$ is independent of $[O_2]$

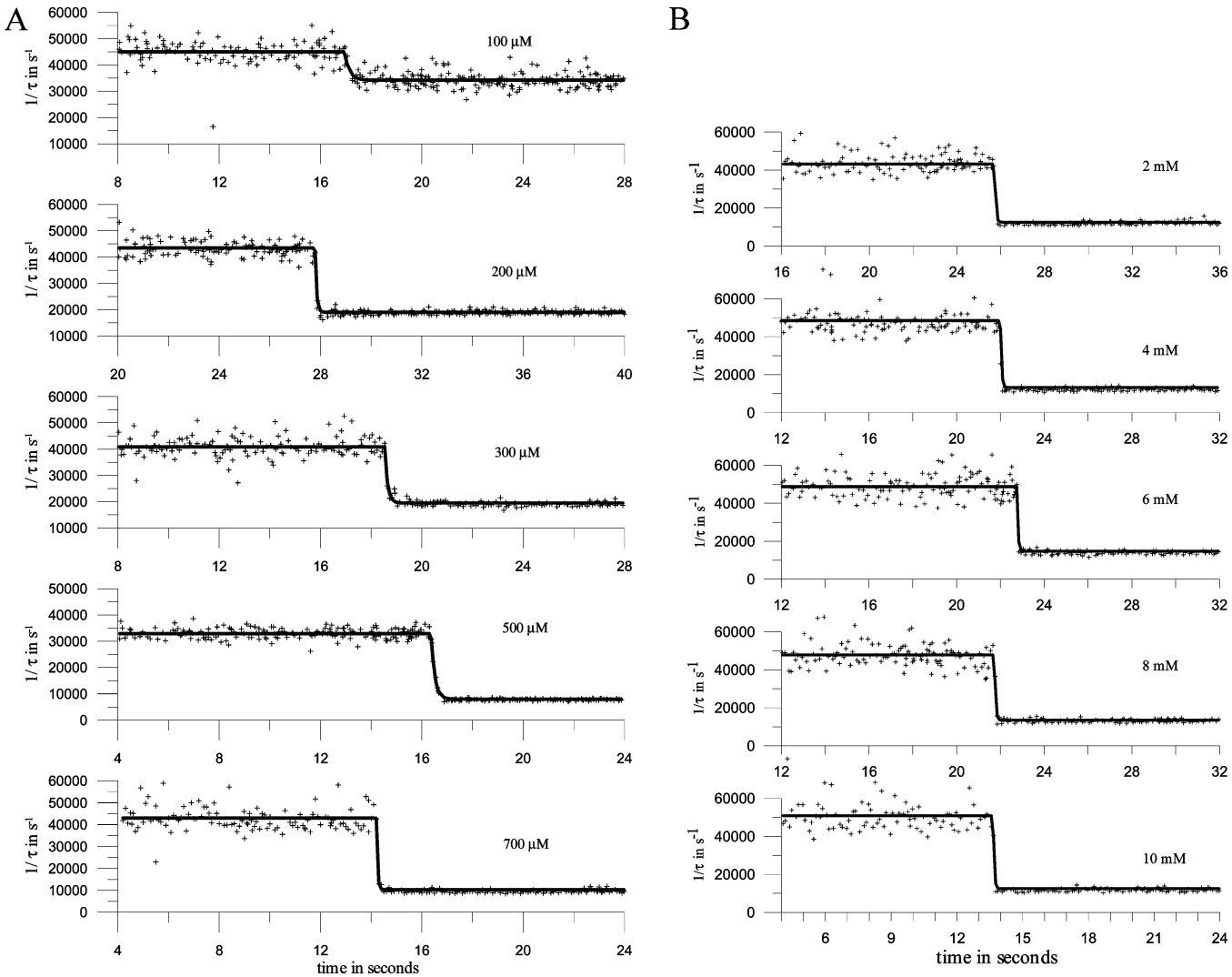

Figure 4. Representative plots (+ signs) of $1/\tau$ vs time obtained by reaction of $S_2O_4^{2-}$ with dissolved O_2 at 37 °C. The reaction (in dH_2O) contained 2.0 μM Pd phosphor, 0.5% albumin, and 100 to 700 μM (A) or 2.0−10.0 mM $S_2O_4^{2-}$ (B). The solid lines are best fits to a horizontal line followed by a decreasing exponential.

(for $[O_2] > 40$ μM) the reaction is apparently zero-order with respect to O_2; where $-d[O_2]/dt$ decreases with $[O_2]$ (for $[O_2] < 40$ μM), the order of the reaction with respect to O_2 is apparently greater than 0. This is consistent with the mechanism of eqs 4 and 5: For higher $[O_2]$, eq 4, which is zero-order in $[O_2]$, is the rate-determining step; but for lower $[O_2]$, eq 5 becomes slower and rate-determining, and it is first-order in $[O_2]$. Creutz and Sutin[6] found $d[O_2]/dt$ to follow zero-order kinetics "over at least 80% reaction" when $S_2O_4^{2-}$ was present in excess. It is also possible that the decrease is exponential, since an exponential is linear close to the origin.

In order to establish the order with respect to $S_2O_4^{2-}$ and to calculate rate constants, we compare the initial rates of reaction r for different $[S_2O_4^{2-}]$. These are calculated according to eq 11 or eq 13. Since the initial rate should be proportional to $[S_2O_4^{2-}]^x[O_2]^0$ where x is the order of the reaction, x can be determined by linear regression on a plot of $\ln(r)$ versus $\ln[S_2O_4^{2-}]$.

Values of r determined from experiments at 25 °C are given in Table 2, and values determined at 37 °C are given in Table 3. Equations 10 and 11, the exponential fitting functions, were used to obtain these values. There was much more scatter in the initial reaction rates at higher T, because of insufficient time resolution in the values of $1/\tau$. In fact, little information is available when the value of $1/\tau$ drops from $1/\tau_b$ at time t to a value indistinguishable from $1/\tau_0$ ($[O_2] \sim 0$) at $t + \Delta t$ where Δt is the time between measurements. Since the standard deviation in $1/\tau$ is $\sim 10^3$ s^{-1} and $1/\tau_b - 1/\tau_0$ is $\sim 3 \times 10^4$ s^{-1}, this means

$$30\, e^{-C\Delta t} < 1$$

or, with $\Delta t = 0.07$ s, $C > 49$ s^{-1}. Thus, values of r are of doubtful validity when

$$r > 3 \times 10^4\, C/k_q = 1.5 \times 10^4\, \mu\text{M s}^{-1}$$

All the values of r in Tables 2 and 3 were used in the fitting; removing those greater than 1.5×10^4 μM s^{-1} changes the results only slightly.

To find the order of the reaction with respect to $S_2O_4^{2-}$, we perform a linear regression of $\ln(r)$ versus $\ln[S_2O_4^{2-}]$, shown in Figure 6. For the 25 °C data, the slope is 0.59 ± 0.07, showing clearly that the reaction is 1/2-order with respect to $S_2O_4^{2-}$. This is expected if eq 4 is the rate-determining step. For 37 °C, the slope is 0.49 ± 0.09 (Figure 6), showing that

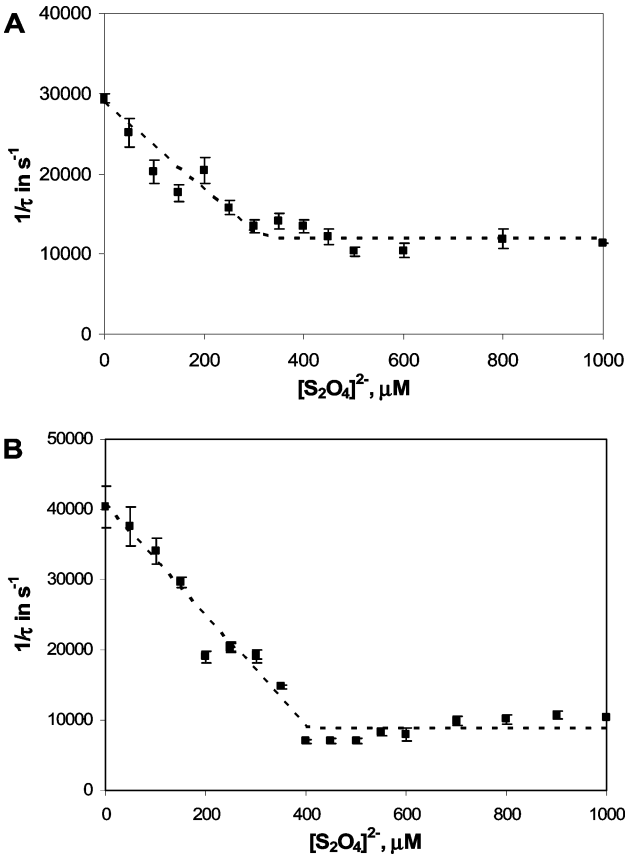

Figure 5. Determinations of stoichiometry of the reaction of $S_2O_4^{2-}$ with O_2 at 25 °C (A) and 37 °C (B). Over 20 data sets with various concentrations of $S_2O_4^{2-}$ below 1.0 mM were obtained. The resulting values of $1/\tau_a$ for some of these data sets are plotted vs $[S_2O_4^{2-}]$, where each error bar is the standard deviation for one determination of $1/\tau_a$. The plot of all $1/\tau_a$ values vs $[S_2O_4^{2-}]$ was fitted to the two-line function shown as a dashed line. The intersection point of the two lines determines the stoichiometry.

the rate-determining step is 1/2-order at the higher temperature as well. We have also calculated r values using eqs 12 and 13, corresponding to fits to a three-line function. Although the values of r are much higher than those in Tables 2 and 3, the slope of a plot of $\ln(r)$ versus $\ln[S_2O_4^{2-}]$ is still ~0.5.

3.4. Rate Constants. In summary, the initial rate of the oxygen-consumption reaction, in μM s^{-1}, is found to be equal to

$$-\frac{d[O_2]}{dt} = \exp(2.092 + 0.594 \ln[S_2O_4^{2-}]) \approx 17.8[S_2O_4^{2-}]^{1/2} \quad (15)$$

at 25 °C and

$$-\frac{d[O_2]}{dt} = \exp(5.124 + 0\ 0.493 \ln[S_2O_4^{2-}]) \approx 196.3[S_2O_4^{2-}]^{1/2} \quad (16)$$

at 37 °C, where $[S_2O_4^{2-}]$ is in μM. Assuming the reaction is first order in O_2 (see below) and using initial concentrations of O_2 of 267 μM at 25 °C and 225 μM at 37 °C, we calculate that the rate constants are 66.7 M$^{-1/2}$ s^{-1} at 25 °C and 872 M$^{-1/2}$ s^{-1} at 37 °C. The temperature dependence of the rate constant corresponds to an activation energy of

$$-R\frac{d\ln(k)}{d(1/T)} = \frac{2.571R}{0.0001298} = 164.7 \text{ kJ/mol}$$

TABLE 2: Initial Rates of Reaction r at 25 °C for Various $[S_2O_4^{2-}]$

$[S_2O_4^{2-}]$, μM	r, μM s^{-1}	$[S_2O_4^{2-}]$, μM	r, μM s^{-1}
50	52	450	755
100	324	500	410
150	394	600	756
200	408	800	358
200	160	1000	423
200	234	1000	286
200	79	1000	161
250	128	2000	698
250	491	3000	942
300	206	4000	487
300	201	5000	1379
300	331	6000	1882
300	157	7000	2754
350	156	8000	3774
350	122	9000	2331
400	177	10000	1232

TABLE 3: Initial Rates of Reaction r at 37 °C for Various $[S_2O_4^{2-}]$

$[S_2O_4^{2-}]$, μM	r, μM s^{-1}	$[S_2O_4^{2-}]$, μM	r, μM s^{-1}
100	566	550	2130
150	3348	600	2499
200	6467	700	8069
250	900	800	2852
250	4549	900	12325
250	4726	1000	7164
300	369	2000	8895
300	4389	3000	9356
300	2041	4000	11859
350	4820	5000	11051
400	3053	6000	10412
450	2633	7000	6519
500	3368	8000	12345
500	14659	9000	11947
500	3246	10000	21854
500	2927		

which should be related to the dissociation energy of $S_2O_4^{2-}$ into $2SO_2^{2-}$. The S−S single-bond energy is 425 kJ/mol;[15] therefore, the S−S bond in dithionite is highly destabilized.

Assuming eqs 4 and 5 are the only reactions contributing to oxygen consumption (note that in the scheme of Rinker et al.,[9] O_2 enters as a reactant in a later step as well), we may write the rate equations as follows. Letting k_1 and k_{-1} be the forward and reverse rate constants for reaction 4 and letting k_2 be therate constant for reaction 5, we find the steady-state equation for the reactive intermediate $\bullet SO_2^-$ is

$$2k_1[S_2O_4^{2-}] - 2k_{-1}[SO_2^-]^2 - k_2[SO_2^-][O_2] = 0 \quad (17)$$

According to Creutz & Sutin[10] $k_1 \sim 2.5$ s^{-1} at pH 8, 25 °C; $k_{-1} \sim 1.8 \times 10^9$ M^{-1} s^{-1} at pH 6.5, 25 °C; $k_2 > 10^8$ M^{-1} s^{-1} 25 °C. If, in our experiments, the second term in eq 17 were much smaller than the third, we would have

$$[SO_2^-] \sim \frac{2k_1[S_2O_4^{2-}]}{k_2[O_2]}$$

and

$$-\frac{d[O_2]}{dt} = k_2[SO_2^-][O_2] = 2k_1[S_2O_4^{2-}]$$

This predicts the order of the reaction with respect to $S_2O_4^{2-}$ incorrectly. Apparently, the second term in eq 17 is larger than

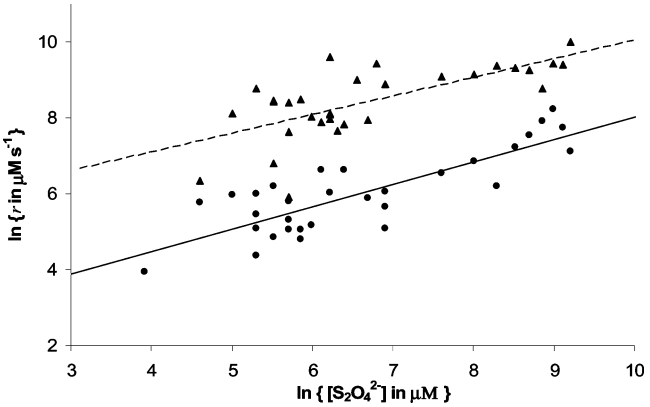

Figure 6. Logarithms of initial rates of the dithionite-oxygen reactions are plotted against logarithms of $[S_2O_4^{2-}]$ at both 25 °C and 37 °C. Linear fits are obtained for the two sets of data. Triangles and the dashed line show the results at 37 °C, whereas dots and the solid line represent the results at 25 °C.

the third, so that $S_2O_4^{2-} \leftrightarrow 2\ SO_2^-$ comes to a rapid equilibrium and

$$-\frac{d[O_2]}{dt} = k_2[SO_2^-][O_2] = k_2\sqrt{\frac{k_1}{k_{-1}}}[S_2O_4^{2-}]^{(1/2)}[O_2] \quad (18)$$

which predicts the order with respect to dithionite correctly. If one accepts this, the order with respect to O_2 is 1, which is also consistent with our observations.

The effective rate constant derived from our results at 25 °C is 66.7 $M^{-1/2}\ s^{-1}$, and this should be equal to $k_2\sqrt{k_1 / k_{-1}}$. It is impossible to use literature values for the rate constants here: the values of k_1 and k_{-1} reported by Creutz and Sutin,[10] were measured at pH 8 and pH 6.5 respectively, while our measurements were at much lower pH. Our measured pH varied linearly with $[S_2O_4^{2-}]$, being 3.61 ± 0.03 for 100 μM and 3.82 ± 0.10 for 10 mM. A value of $2.4 \times 10^9\ M^{-1}\ s^{-1}$ was reported by Huie et al[16] for

$$\bullet SO_2^- + O_2 \rightarrow SO_2 + \bullet O_2^- \quad (19)$$

at room temperature, pH = 1.0. It seems very likely that eq 19 is the first reaction in the series of reactions indicated by eq 5. Note that SO_2 in aqueous solution near neutral pH is equivalent to bisulfite, so that bisulfate must be formed by subsequent reactions. For example, superoxide ion O_2^- (like O_2) can oxidize S(iv) to S(v),[17] which is easily oxidized to S(vi) (bisulfate).

4. Conclusions

From the above results, it can be seen that our instrument can be conveniently utilized to monitor rapid chemical reactions, by measuring the phosphorescence decay rate, $1/\tau$. Since $1/\tau$ is linearly dependent on $[O_2]$, measurement of $1/\tau$ gives $[O_2]$.[1−4,18−23] The tail of each phosphorescence decay profile was fit to an exponential function to measure $[O_2]$. Presently, phosphorescence profiles are obtained every 0.1 s (flash rate), making it feasible to monitor chemical reactions in which the oxygen concentration changes substantially in a few hundred milliseconds. Reactions 100 times faster could be tracked if the flash rate were increased to 1000 Hz.

We applied our O_2 analyzer to investigate the reaction of $S_2O_4^{2-}$ with O_2, which apparently begins with the reactions of eqs 4 and 5. The stoichiometry study shows 1.2:1.0 ($S_2O_4^{2-}$/O_2) at 25 °C (consistent with the results of other workers) and 1.6:1.0 at 37 °C. The variation may be due to different temperature dependences of the rates of the reaction steps which follow eq 5. The relative rates of these steps determine the overall stoichiometry and, equivalently, the relative amounts of bisulfate and bisulfate produced. The reaction of SO_2^- with O_2 very probably produces SO_2 and O_2^-, and SO_2 in aqueous solution already yields HSO_3^-. Subsequent reactions involve further oxidations by O_2 and O_2^-.

The kinetics study shows that at both temperatures the oxygen depletion $-d[O_2]/dt$ is $^1/_2$-order in $[S_2O_4^{2-}]$ and first-order in $[O_2]$. This supports the suggestion of previous workers that conversion between $S_2O_4^{2-}$ and SO_2^- (eq 4) reaches equilibrium rapidly, so that reaction 5 is rate-determining and is the main contributor to the depletion of oxygen.

Acknowledgment. This work is supported by a fund from the Paige's Butterfly Run. We appreciate the contribution of Dr. Harvey Penefsky, who built the apparatus and allowed us to use it for these measurements. We also appreciate the contribution of Dr. Yu Zhang with the electronic circuit and of Mr. Shiliyang Xu with the computer language.

References and Notes

(1) Vanderkooi, J. M.; Wilson, D. F. *Adv. Exp. Med. Biol.* **1986**, *200*, 189.
(2) Rumsey, W. L.; Vanderkooi, J. M.; Wilson, D. F. *Science* **1988**, *241*, 1649.
(3) Wilson, D. F. *Adv. Exp. Med. Biol.* **1992**, *317*, 195.
(4) Pawlowski, M.; Wilson, D. F. *Adv. Exp. Med. Biol.* **1992**, *316*, 179.
(5) Tao, Z.; Withers, H. G.; Penefsky, H. S.; Goodisman, J.; Souid, A.-K. *Chem. Res. Toxicol.* **2006**, *19*, 1051.
(6) Tao, Z.; Ahmad, S. S.; Penefsky, H. S.; Goodisman, J.; Souid, A.-K. *Mol. Pharmaceutics* **2006**, *3*, 762.
(7) Tao, Z.; Penefsky, H. S.; Goodisman, J.; Souid, A.-K. *Mol. Pharmaceutics* **2007**, *4*, 583.
(8) Quiggle, D. *Ind. Eng. Chem.* **1936**, *5*, 393.
(9) Rinker, R. G.; Gordon, T. P.; Mason, D. M.; Sakaida, R. R.; Corcoran, W. H. *J. Phys.Chem.* **1960**, *64*, 573.
(10) Creutz, C.; Sutin, N. *Inorg. Chem.* **1974**, *13*, 2041.
(11) Simon, A.; Kuchler, H. *Z. Anorg. Chem.* **1949**, *260*, 161.
(12) Dunitz, J. D. *Acta. Cryst.* **1956**, *9*, 579.
(13) Kawagoe, M.; Robinson, C. W. *Can. J. Chem. Eng.* **1981**, *59*, 471.
(14) Vanderkooi, J. M.; Maniara, G.; Green, T. J.; Wilson, D. F. *J. Biol. Chem.* **1987**, *262*, 5476.
(15) *Handbook of Chemistry and Physics*; Chemical Rubber Publishing Co.; Table 9, p 58.
(16) Huie, R. E.; Clifton, C. L.; Altstein, N. *Radiat. Phys. Chem.* **1989**, *33*, 361.
(17) Weinstein-Lloyd, J.; Schwartz, S. E. *Environ. Sci. Technol.* **1991**, *25*, 791.
(18) Lo, L. W.; Koch, C. J.; Wilson, D. F. *Anal. Biochem.* **1996**, *236*, 153.
(19) Clark, H. A.; Hoyer, M.; Parus, S.; Philbert, M. A.; Kopelman, R. *Microchim. Acta* **1999**, *131*, 121.
(20) Wilson, D. F.; Rumsey, W. L.; Vanderkooi, J. M. *Adv. Exp. Med. Biol.* **1989**, *248*, 109.
(21) Vanderkooi, J. M.; Erecinska, M.; Silver, I. A. *Am. J. Physiol.* **1991**, *260*, C1131.
(22) Wilson, D. F.; Cerniglia, G. J. *Cancer Res.* **1992**, *52*, 3988.
(23) Vinogradov, S. A.; Wilson, D. F. *Adv. Exp. Med. Biol.* **1997**, *428*, 657.